CHAPTER THREE
ESDM TECHNIQUE

ESDM is a technique which reconstructs three-dimensional velocity fields associated with vibrating structures using spatially dense velocity measurements obtained from a scanning LDV. The ability to reconstruct such velocity fields is an extremely powerful structural dynamics analysis tool which greatly enhances the usefulness of a scanning LDV. This chapter provides a detailed explanation of ESDM including its capabilities, its implementation using a scanning LDV and its theoretical foundation. However, the reader who is familiar with ESDM may continue directly to the next chapter which discusses LDV scanner calibration.

Nomenclature

$\boldsymbol{a}$	acceleration vector
$[\boldsymbol{A}]_v$	matrix
b_f	force signal coefficient
b_{f_c}	force signal cosine coefficient
b_{f_o}	force signal offset constant
b_{f_s}	force signal sine coefficient
b_v	velocity signal coefficient
b_{v_c}	velocity signal cosine coefficient
b_{v_o}	velocity signal offset constant
b_{v_s}	velocity signal sine coefficient
$\hat{b}_v$	regressed velocity signal coefficient
$\hat{b}_{v_c}$	regressed velocity signal cosine coefficient
$\hat{b}_{v_o}$	regressed velocity signal offset constant
$\hat{b}_{v_s}$	regressed velocity signal sine coefficient
d	differential operator
$\boldsymbol{d}$	displacement vector
e	error term
$\boldsymbol{e}_v$	error vector

f	force magnitude
$\boldsymbol{f}$	effective nodal force vector
i	index
j	index
k	index
l	number of elements
$[\boldsymbol{K}]$	element effective dynamic stiffness matrix
m	number of element nodes
n	number of scan points
N	element interpolating function
O	laser beam virtual origin
O_L	LDV coordinate system origin
O_S	structure coordinate system origin
O_{L_S}	LDV coordinate system origin in structure coordinate system
P	arbitrary point illuminated by laser beam
$\boldsymbol{r}$	position vector from laser beam virtual origin to arbitrary point illuminated by laser beam
$\boldsymbol{r}_L$	position vector from LDV coordinate system origin to arbitrary point illuminated by laser beam
$\bar{\boldsymbol{r}}_{\boldsymbol{S}}$	unit vector associated with position vector from structure coordinate system origin to arbitrary point illuminated by laser beam
$\boldsymbol{r}_O$	position vector from LDV coordinate system origin to laser beam virtual origin
$\boldsymbol{r}_{O_{L_S}}$	position vector of LDV coordinate system origin in structure coordinate system
$\boldsymbol{r}_S$	position vector from LDV coordinate system origin to arbitrary point illuminated by laser beam
$[\boldsymbol{R}]_{L\rightarrow S}$	rotation matrix from LDV coordinate system to structure coordinate system
t	time
$\boldsymbol{T}_{\boldsymbol{O}\rightarrow\boldsymbol{O}_L}$	translation vector from laser beam virtual origin to LDV coordinate system origin
$\boldsymbol{T}_{\boldsymbol{O}_L\rightarrow\boldsymbol{O}_S}$	translation vector from LDV coordinate system origin to structure coordinate system origin
v	velocity magnitude
$\boldsymbol{v}$	velocity vector
v_c	velocity magnitude cosine coefficient
v_s	velocity magnitude sine coefficient
$\boldsymbol{v}_c$	velocity vector cosine coefficient
$\boldsymbol{v}_s$	velocity vector sine coefficient
$\boldsymbol{v}_L$	velocity vector aligned with LDV laser beam direction

$\bar{\boldsymbol{v}}_L$	unit vector corresponding to velocity vector aligned with LDV laser beam direction
x, y, z	spatial Cartesian coordinates; spatial Cartesian components
x_L, y_L, z_L	spatial LDV coordinate system Cartesian coordinates
x_S, y_S, z_S	structure coordinate system Cartesian coordinates
$[\boldsymbol{\Gamma}]_{L\rightarrow S}$	transformation matrix from LDV coordinate system to structure coordinate system
ε	error term
ξ, ζ, η	parametric element coordinates
θ_H	horizontal scan angle
θ_V	vertical scan angle
Π	summation of weighted, squared errors
σ	residual error variance
Ψ_L	direction cosine
ϕ_v	velocity signal phase
ϕ_f	force signal phase
ϕ_r	relative phase between velocity and force signals
$\boldsymbol{\Phi}$	angle between velocity vector aligned with laser beam direction and true velocity vector at same structure point
ω	circular frequency
Σ	summation operator
^{T}	transpose operator

ESDM Capabilities

As currently developed, ESDM is capable of reconstructing steady-state, continuous, three-dimensional, surface velocity fields resulting from single frequency, harmonic, temporal excitations. If a linear relationship between response and excitation is assumed, the velocity field is also harmonic at the excitation frequency. Since both the velocity field and excitation are harmonic and since the velocity response is causal with respect to the excitation, the continuous velocity response lags the excitation by a continuously varying, spatially dependent phase angle. ESDM accounts for this phase relationship.

Velocity field reconstruction is based upon a finite element formulation. However, unlike traditional finite element formulations which minimize a particular theoretical relation derived from a differential equation such as the variational description of potential energy in structural mechanics, the finite element formulation employed by ESDM minimizes the least-squares error between experimentally obtained LDV velocity data and the modeled velocity field. Such a finite element formulation is advantageous for several reasons [10,11]. First, it enables the analysis of structures possessing complex geometry. Second, it solves the velocity field, both magnitude and direction, simultaneously instead of piecemeal. Third, such a formulation retains all statistical information associated with the experimental LDV velocity data, thereby allowing statistical qualification of resulting velocity field solutions. Fourth, it allows modeling of both geometry and velocity simultaneously. Each element uses interpolation polynomials which describe the variation of surface geometry and velocity within each element. As a result, the resulting velocity field solution is not obtained independently of the structure geometry. Last, the accuracy of the reconstructed velocity field may be controlled by the number of elements used to discretize the geometry and the order of the element interpolation polynomials used.

Once the velocity field solution is obtained, solution processing software included with ESDM allows visualization of the velocity field. Velocity magnitude, direction and phase may be displayed and animated. Solution statistical properties may also be obtained. In addition, other fields are constructed from the velocity field solution. Displacement, strain and acceleration fields are all derived and may be displayed.

General ESDM Procedure

ESDM begins with the creation of a finite element mesh which provides the geometric model of the structure being analyzed. This model serves two purposes: 1) by modeling the structure geometry, it provides a method for determining surface geometry variation, thereby providing a method for ultimately determining velocity direction and 2) it serves as the basis for the velocity field finite element model since the same elements used to model geometry are used to model velocity. The mesh may be created using either a commercial finite element software package for geometrically complex structures or ESDM software for less complex geometry.

After the finite element model is completed, the pose (position and orientation) of the scanning LDV used to acquire velocity data is determined relative to the structure. This process, termed registration, is extremely important since the LDV measures velocity only along the direction of the laser beam at each structure point illuminated by the laser; that is, at each scan point. Once the LDV pose is known, direction cosines between a vector describing laser beam direction, referenced to the structure coordinate system, and a vector describing scan point position, also referenced to the structure coordinate system, are determined. These direction cosines are integral to determining velocity field direction. After registration, the LDV scans the structure and measures velocity at multiple scan points over a specified period of time. For velocity field reconstruction, at least three scan points within each element are required and the time duration over which velocity data is collected must include at least one full cycle of motion. Usually, the LDV is directed, via scanning software, to scan a rectangular area

superimposed on the structure in a uniform manner. At least three different, well separated, non-coplanar LDV scan positions are mathematically required to determine velocity direction [12]; therefore, registration and scanning must be conducted at least three different times. LDV registration issues are discussed in greater detail later in this chapter.

Once registration is completed, the structure is scanned by the LDV and velocity measured at each scan point. A computer program included with the ESDM software suite processes the discrete velocity data collected by the LDV. Data processing at this stage entails continuous time-domain reconstruction of the velocity signal from the discrete velocity samples obtained at each scan point. A detailed explanation of time-domain reconstruction is included as a later section in this chapter.

After time-domain reconstruction, other computer programs, which contain the structure geometry and velocity finite element formulations, reconstruct the continuous, three-dimensional, translational velocity field. In addition to LDV registration and velocity time-signal reconstruction, the least-squares finite element formulation employed by ESDM is discussed in more detail later in this chapter.

Once the velocity field solution is obtained, it may be statistically validated. Residual errors between the LDV velocity data and the resulting velocity field are determined. Residual error variance is calculated as is the ratio between velocity field magnitude and residual error at each scan point.

The velocity field solution is actually a translational velocity field. Further processing of the solution yields the rotational velocity field. Moreover, other fields may

be derived including the translational and rotational displacement fields, the translational and rotational acceleration fields and, based upon certain assumptions, the strain and stress fields.

Last, solution analysis is conducted. As mentioned before, solution processing software included with the ESDM software suite allows visualization of reconstructed velocity fields. Translational and rotational velocity fields, including magnitude, direction and phase information, may be displayed and animated as well as solution statistical properties. In addition, other fields derived from the velocity field may be viewed such as the displacement, acceleration, strain and stress fields.

LDV Registration

LDV registration is required before each scan in order to determine LDV pose relative to a user-defined Cartesian coordinate system associated with the structure being analyzed. LDV pose is required to determine laser beam direction at each velocity measurement point on the structure. Once this direction is determined, direction cosines between the laser beam vector direction and the scan point vector direction are determined. Both vectors are referenced to the structure coordinate system. Ultimately, the velocity direction is determined.

Mathematically, registration involves the calculation of a transformation matrix which provides a way to transform laser beam direction information referenced with respect to a LDV coordinate system to the structural coordinate system. ESDM accomplishes this task using a multiple-point, indirect registration algorithm also developed by Montgomery [13].

Before describing the indirect registration algorithm, the scanning operation of a scanning LDV must be explained. A scanning LDV utilizes two scanners which deflect the laser beam horizontally or vertically. Each scanner is composed of a mirror and a rotational galvanometer. The mirror is rotated by the galvanometer in response to an analog voltage signal. A typical scanner mounting configuration is shown in Fig. 1. Rotation of the bottom mirror deflects the laser beam horizontally; similarly, rotation of the top mirror deflects the laser beam vertically. The locus of points which constitute the laser beam virtual origin is also shown in Fig. 1. If only the bottom mirror is rotated and

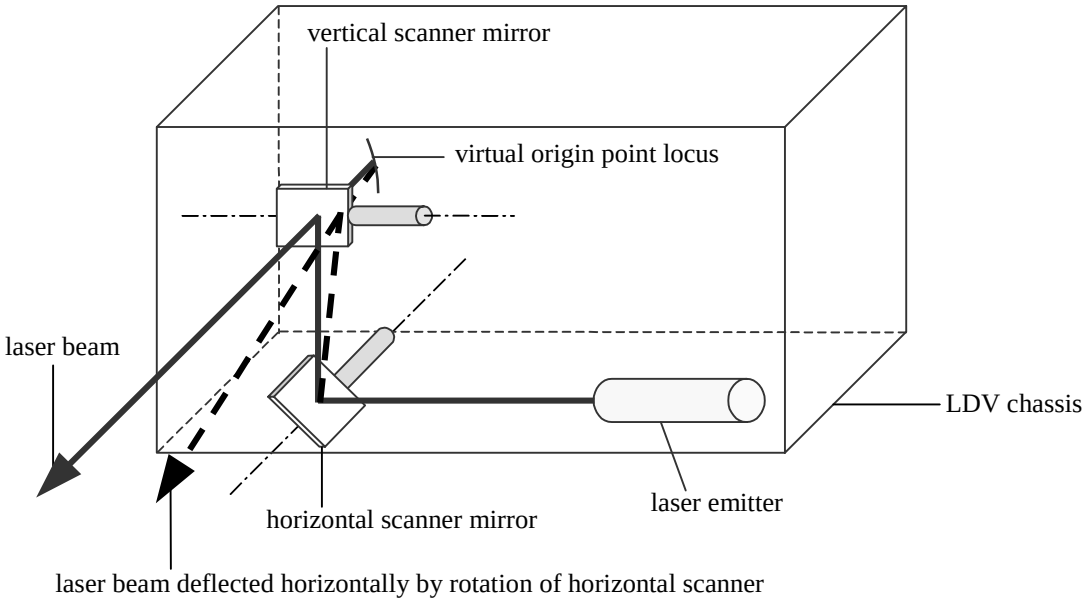

Figure 1. Typical scanner mounting configuration

the mirror reflective surface coincides with the mirror axis of rotation, the laser beam virtual origin is located at a stationary point behind the vertical mirror centerline at a distance equal to the separation between the horizontal and vertical mirrors; if only the top mirror is rotated and the mirror reflective surface coincides with the mirror rotation

axis, the laser beam virtual origin is located at the vertical mirror centerline. If both mirrors are rotated, as occurs during a typical scan, the virtual origin traces an arc with a centerline at the vertical mirror center and a radius behind the vertical mirror centerline equal to the separation distance between the two mirrors.

The horizontal and vertical angles through which the laser beam is deflected by the scanners are called scan angles. The scanners are actuated by analog voltages which range between equal positive and negative values. At zero voltage for each scanner, the laser beam is at its home position. All scan angles are referenced to this home position as shown in Fig. 2. In Fig. 2, the horizontal scan angle is θ_H, the vertical scan angle is θ_V and P is a point illuminated by the laser beam. Maximum horizontal and vertical scan angles for typical scanners range from 12° to 20°. The horizontal and vertical scan angles partially define an LDV Cartesian coordinate system which is used to reference laser beam direction. The additional parameters needed to fully define this coordinate system are distance (range) from the virtual origin to the point on the structure illuminated by the laser and the location of the virtual origin with respect to a fixed point on the LDV chassis.

Mathematical development of the transformation matrix involves the following steps. First, considering Fig. 3, the scan angles and range from the virtual origin to an arbitrary point illuminated by the laser are converted to components along three orthogonal axes aligned with the LDV Cartesian coordinate system by the following relation:

$$\boldsymbol{r} = \begin{Bmatrix} r\cos\theta_V \sin\theta_H \\ r\sin\theta_V \\ r\cos\theta_V \cos\theta_H \end{Bmatrix}. \tag{1}$$

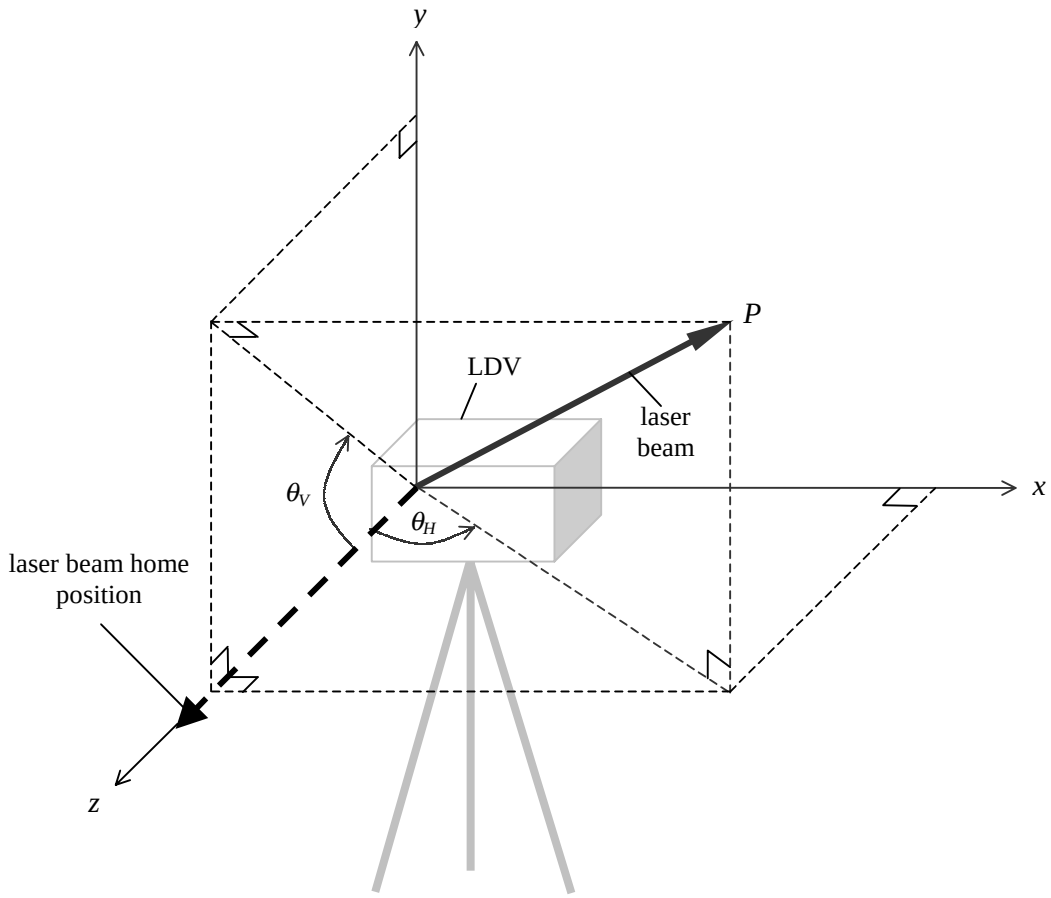

Figure 2. Horizontal and vertical scan angles defined

Second, the laser virtual origin is translated to the fixed point on the LDV chassis which serves as the LDV coordinate system. Information regarding the locations of mirror rotational axes relative to the fixed reference point and the separation distance between these axes is usually available from the LDV manufacturer. These locations and the separation distance are needed to determine the virtual origin location with respect to the

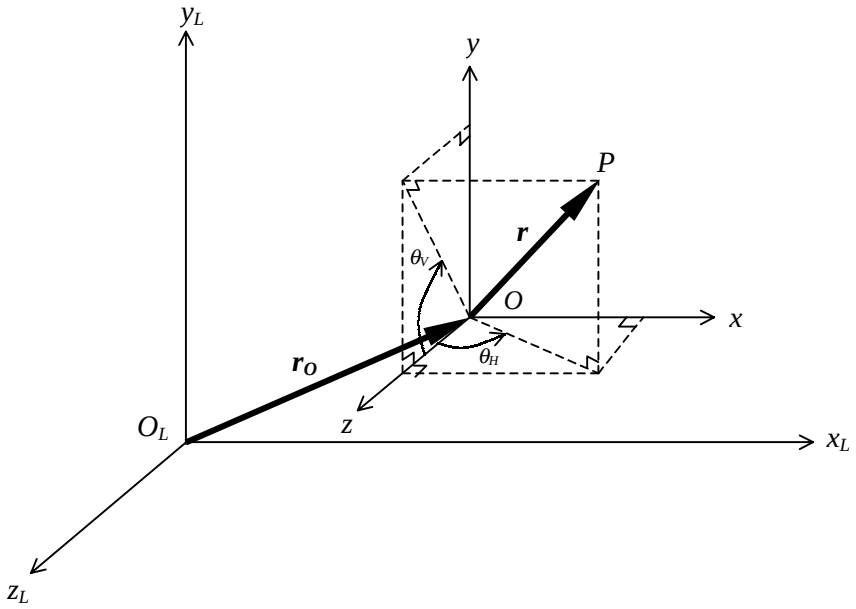

Figure 3. Position vectors which define the location of an arbitrary scan point illuminated by the laser beam in the LDV coordinate system

fixed reference point. Mathematically, considering Fig. 3 again, the virtual origin translation in LDV coordinates is

$$\boldsymbol{T}_{\boldsymbol{O}\to O_L} = -\boldsymbol{r_O} = -\begin{Bmatrix} O_{x_L} \\ O_{y_L} \\ O_{z_L} \end{Bmatrix}. \tag{2}$$

Equations (1) and (2) together define the arbitrary point in the LDV Cartesian coordinate system:

$$\boldsymbol{r}_L = \boldsymbol{r} + \boldsymbol{T}_{\boldsymbol{O}\to \boldsymbol{O_L}} = \begin{Bmatrix} r\sin\theta_H \cos\theta_V - O_{x_L} \\ r\sin\theta_V - O_{y_L} \\ r\cos\theta_H \cos\theta_V - O_{z_L} \end{Bmatrix}. \tag{3}$$

Third, considering Fig. 4, the LDV coordinate system is transformed into the structural coordinate system. The transformation involves 1) a translation of the LDV origin to the

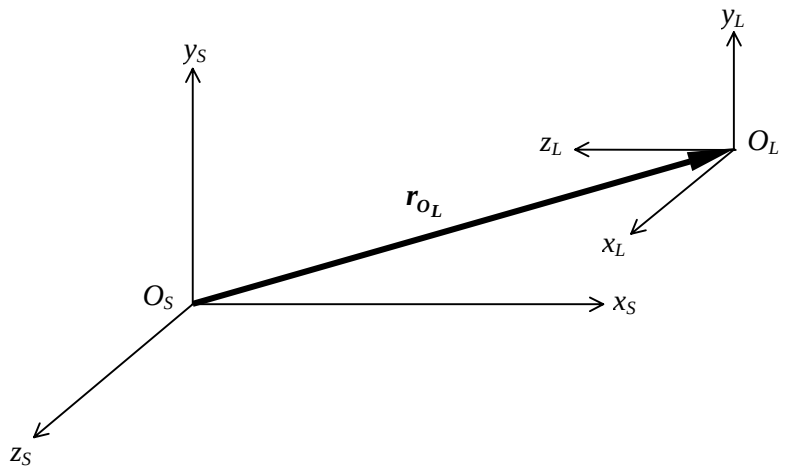

Figure 4. Relationship between LDV and structure coordinate systems

structural origin and 2) a rotation of the LDV system to align it with the structural system. Mathematically, the translation is

$$\boldsymbol{T}_{\boldsymbol{O_L}\rightarrow O_S} = -\boldsymbol{r}_{\boldsymbol{O_L}} = -\begin{Bmatrix} O_{L_{xS}} \\ O_{L_{yS}} \\ O_{L_{zS}} \end{Bmatrix}. \tag{4}$$

This equation is expanded in matrix form as [14]

$$[\boldsymbol{T}]_{\boldsymbol{O}_L\rightarrow O_S} = \begin{bmatrix} 1 & 0 & 0 & -O_{L_{xS}} \\ 0 & 1 & 0 & -O_{L_{yS}} \\ 0 & 0 & 1 & -O_{L_{zS}} \\ 0 & 0 & 0 & 1 \end{bmatrix}. \tag{5}$$

The rotation is represented by $[\boldsymbol{R}]_{L\rightarrow S}$, a 3x3 rotation matrix whose development is discussed by Montgomery [15] and Zeng [16]. This matrix is expanded into a 4x4 matrix to accommodate multiplication with the translation matrix given by Eq. (5). The expansion is

$$[\boldsymbol{R}]_{L\to S} = \begin{bmatrix} & & & 0 \\ & [\boldsymbol{R}_{L\to S}]_{3x3} & & 0 \\ & & & 0 \\ 0 & 0 & 0 & 1 \end{bmatrix}. \tag{6}$$

Multiplying Eqs. (5) and (6) yields the desired transformation matrix:

$$[\boldsymbol{\Gamma}]_{L\to S} = \begin{bmatrix} & & & -O_{L_{xS}} \\ & [\boldsymbol{R}_{L\to S}]_{3x3} & & -O_{L_{yS}} \\ & & & -O_{L_{zS}} \\ 0 & 0 & 0 & 1 \end{bmatrix}. \tag{7}$$

Basically, the goal of LDV registration is to determine the relationship, described by the transformation matrix, $[\boldsymbol{\Gamma}]_{L\to S}$, between the LDV and structure coordinate systems. Ultimately, the transformation matrix allows the laser beam direction to be determined relative to the structure coordinate system. Unlike other registration methods such as direct registration, multiple-point, indirect registration does not use range information from the laser virtual origin to registration points illuminated by the laser. Therefore, multiple-point indirect registration is more general since range information is not always available. Recall, however, that this range information, along with the scan angles and location of the virtual origin with respect to the LDV coordinate system origin, is needed to fully define the LDV coordinate system. The indirect method overcomes this problem by employing the following concept. Consider a set of points, formally termed registration points, referenced to the structure coordinate system. Also, consider these same points referenced to the LDV coordinate system. A transformation of registration point coordinate values from the LDV coordinate system to the structure coordinate system should yield the original structure coordinate system values. Using this concept,

multiple-point indirect registration employs an algorithm which iterates through various range values until a combined squared error described by Montgomery [17] is minimized. Minimization of the combined error with at least four non-collinear registration points yields a unique solution for the desired transformation matrix, $[\boldsymbol{\Gamma}]_{L\to S}$.

Time-Domain Velocity Signal Reconstruction

The scanning LDV scans a structure measuring velocity at multiple structural points. At each point scanned, the velocity signal obtained from the LDV is sampled discretely and collected by an analog-to-digital (A/D) signal conversion unit. ESDM software, using a multiple linear, least squares regression algorithm, then processes this discrete signal to obtain a continuous, time-domain representation of the velocity response at each scan point [18].

Before discussing the multiple linear, least squares regression algorithm employed by ESDM, mathematical, time-domain descriptions of the velocity response and corresponding excitation must be developed. Assuming the independence of temporal and spatial solution components, the continuous, three-dimensional velocity field is separable as

$$v(x,y,z,t) = v(t)\mathbf{v}(x,y,z)\,, \tag{8}$$

where $v(t)$ is the temporal component and $\mathbf{v}(x,y,z)$ is the spatial component referred to some Cartesian coordinate system. Recall that the time-domain component of the velocity field is steady-state and harmonic at a single frequency; it is represented as

$$v(t) = b_{v_o} + b_v \cos(\omega t - \phi_v)\,. \tag{9}$$

Expanding Eq. (9) yields separate cosine and sine components:

$$v(t) = b_{v_o} + b_v \cos\phi_v \cos(\omega t) + b_v \sin\phi_v \sin(\omega t); \tag{11}$$

or in terms of cosine and sine coefficients:

$$v(t) = b_{v_o} + b_{v_c} \cos(\omega t) + b_{v_s} \sin(\omega t), \tag{12}$$

where the cosine coefficient is

$$b_{v_c} = b_v \cos\phi_v \tag{13}$$

and the sine coefficient is

$$b_{v_s} = b_v \sin\phi_v . \tag{14}$$

Similarly, the excitation, usually a force supplied by a shaker and measured with a force transducer, is represented as a single-frequency, steady-state, harmonic function:

$$f(t) = b_{f_o} + b_f \cos(\omega t - \phi_f). \tag{15}$$

Expanding Eq. (15) into separate cosine and sine parts yields

$$f(t) = b_{f_o} + b_{f_c} \cos(\omega t) + b_{f_s} \sin(\omega t), \tag{16}$$

where the cosine coefficient is

$$b_{f_c} = b_f \cos\phi_f \tag{17}$$

and the sine coefficient is

$$b_{f_s} = b_f \sin\phi_f . \tag{18}$$

Multiple linear, least squares regression is used to reconstruct the velocity response and excitation signals. Directly from Eq. (12), the velocity response is

$$v(t_i) = b_{v_o} + b_{v_c} \cos(\omega t_i) + b_{v_s} \sin(\omega t_i). \tag{19}$$

This is the equation which will be modeled using multiple linear regression. The equation resulting from the regression is an approximation of Eq. (19); it is

$$v(t_i) \cong \hat{b}_{v_o} + \hat{b}_{v_c} \cos(\omega t_i) + \hat{b}_{v_s} \sin(\omega t_i). \tag{20}$$

Adding a residual error term to Eq. (20) yields

$$v(t_i) = \hat{b}_{v_o} + \hat{b}_{v_c} \cos(\omega t_i) + \hat{b}_{v_s} \sin(\omega t_i) + \varepsilon_i \tag{21}$$

which is an exact representation of the velocity response at each sample point originally specified by Eq. (19). In matrix form for *n* velocity samples, the previous equation yields

$$\boldsymbol{v} = [\boldsymbol{A}]_v \hat{\boldsymbol{b}}_v + \boldsymbol{e}_v, \tag{22}$$

where

$$\boldsymbol{v} = \begin{Bmatrix} v(t_1) \\ v(t_2) \\ \vdots \\ v(t_n) \end{Bmatrix}, \tag{23}$$

$$[\boldsymbol{A}]_v = \begin{bmatrix} 1 & \cos(\omega t_1) & \sin(\omega t_1) \\ 1 & \cos(\omega t_2) & \sin(\omega t_2) \\ \vdots & \vdots & \vdots \\ 1 & \cos(\omega t_n) & \sin(\omega t_n) \end{bmatrix}, \tag{24}$$

$$\hat{\boldsymbol{b}}_v = \begin{Bmatrix} \hat{b}_{v_o} \\ \hat{b}_{v_c} \\ \hat{b}_{v_s} \end{Bmatrix} \tag{25}$$

and

$$\boldsymbol{e}_v = \begin{Bmatrix} \varepsilon_1 \\ \varepsilon_2 \\ \vdots \\ \varepsilon_n \end{Bmatrix}. \tag{26}$$

Rearranging Eq. (22) yields

$$\boldsymbol{e}_v = \boldsymbol{v} - [\boldsymbol{A}]_v \hat{\boldsymbol{b}}_v . \tag{27}$$

Squaring the previous equation in matrix form yields a sum of the squared errors which is then minimized and subsequently yields estimates for the offset and the cosine and sine coefficients in Eq. (19). Squaring Eq. (27) yields

$$\boldsymbol{e}_v^T \boldsymbol{e}_v = \boldsymbol{v}^{\mathrm{T}} \boldsymbol{v} - 2\boldsymbol{v}^{\mathrm{T}} [\boldsymbol{A}]_v \hat{\boldsymbol{b}}_v^{\mathrm{T}} + \hat{\boldsymbol{b}}_v^{\mathrm{T}} [\boldsymbol{A}]_v^{\mathrm{T}} [\boldsymbol{A}]_v \boldsymbol{b}_v . \tag{28}$$

Minimizing the sum of the squared errors entails taking the partial derivative of Eq. (28) with respect to the coefficient vector and setting the result equal to zero. This operation yields

$$\frac{\partial}{\partial \hat{\boldsymbol{b}}_v} \left(\boldsymbol{e}_v^{\mathrm{T}} \boldsymbol{e}_v \right) = 2[\boldsymbol{A}]_v^{\mathrm{T}} [\boldsymbol{A}]_v \hat{\boldsymbol{b}}_v - 2\boldsymbol{v}^{\mathrm{T}} [\boldsymbol{A}]_v^{\mathrm{T}} . \tag{29}$$

Solving for the vector of coefficients yields estimates for the offset and cosine and sine coefficients in Eq. (19):

$$\hat{\boldsymbol{b}}_v = \left([\boldsymbol{A}]_v^{\mathrm{T}} [\boldsymbol{A}]_v \right)^{-1} [\boldsymbol{A}]_v^{\mathrm{T}} \boldsymbol{v}^{\mathrm{T}} . \tag{30}$$

Estimates for the offset and cosine and sine coefficients for the excitation signal in Eq. (16) are determined by the same approach.

Once velocity response regressions are completed at each scan point and the excitation regression is completed, various statistical tests are performed to determine

whether the regressions are valid [19]. First, the velocity response and excitation residual errors are analyzed to determine whether unexplained error not attributable to regression is present. Specifically, the residual error variance is analyzed. Large error variance indicates poor quality data, thus invalidating the regression. Second, the probability that regression approximates the sampled signals is evaluated by a statistical *F* test which provides a means for comparing the variances of two normally distributed random variables [20]. In this case, the *F* test is used to compare the regression variance with the residual error variance. A residual error variance greater than the regression variance indicates a low probability that the particular regression is valid. Third, correlation is evaluated between the velocity response and excitation to determine whether the velocity response corresponds to the excitation. Low correlation indicates the velocity response is not related to the excitation. Therefore, the linear relationship between velocity response and excitation is violated, and the regression is invalid.

Once the regressions are deemed valid, the velocity response is referenced to the excitation [21]. This is done to provide a phase reference for the velocity response. Recall that the velocity response is

$$v(t) = b_{v_o} + b_v \cos(\omega t - \phi_v). \tag{31}$$

Then, the velocity response referenced to the excitation is

$$v(t) = b_{v_o} + b_v \cos(\omega t - \phi_r), \tag{32}$$

where

$$\phi_r = \phi_v - \phi_f, \tag{33}$$

where

$$\phi_v = \tan^{-1}\left(\frac{b_{v_s}}{b_{v_c}}\right), \tag{34}$$

and

$$\phi_f = \tan^{-1}\left(\frac{b_{f_s}}{b_{f_c}}\right). \tag{35}$$

Expanding Eq. (27) in terms of cosine and sine coefficients yields

$$v(t) = b_{v_o} + b_{v_c}\cos(\omega t) + b_{v_s}\sin(\omega t), \tag{36}$$

where

$$b_{v_c} = b_v \cos\phi_r \tag{37}$$

and

$$b_{v_s} = b_v \sin\phi_r . \tag{38}$$

This equation defines the temporal component of the velocity field at each LDV scan point.

ESDM Finite Element Formulation

ESDM uses a least-squares finite element formulation to reconstruct the velocity field [22]. Unlike traditional finite element formulations which minimize a particular, physical variational statement, the finite element formulation employed by ESDM minimizes the squared error between the LDV velocity data and the modeled velocity field. Actually, ESDM uses a weighted, least-squares finite element formulation; the residual error variances obtained from the velocity response time-domain, regression weight the squared error term which is then minimized.

Before discussing the actual finite element formulation, the modeled velocity field must be presented. Recall from Eq. (8) that the mathematical model for the continuous, three-dimensional velocity field is

$$\boldsymbol{v}(x, y, z, t) = v(t)\boldsymbol{v}(x, y, z), \tag{39}$$

where, again, $v(t)$ is the temporal component and $\boldsymbol{v}(x,y,z)$ is the spatial component referred to some Cartesian coordinate system. The time-domain component is a steady-state, harmonic, single-frequency function referenced to the excitation as given by Eq. (32). Therefore, neglecting the offset term, Eq. (39) becomes

$$\boldsymbol{v}(x, y, z, t) = \{b_v(x, y, z)\cos[\omega t - \phi_r(x, y, z)]\}\boldsymbol{v}(x, y, z) \tag{40}$$

or in terms of cosine and sine coefficients

$$\boldsymbol{v}(x, y, z, t) = [b_{v_c}(x, y, z)\cos(\omega t) + b_{v_s}(x, y, z)\sin(\omega t)]\boldsymbol{v}(x, y, z). \tag{41}$$

This equation yields

$$\boldsymbol{v}(x, y, z, t) = \boldsymbol{v}_c(x, y, z)\cos(\omega t) + \boldsymbol{v}_s(x, y, z)\sin(\omega t), \tag{42}$$

where

$$\boldsymbol{v}_c(x, y, z) = b_{v_c}(x, y, z)\boldsymbol{v}(x, y, z) \tag{43}$$

and

$$\boldsymbol{v}_s(x, y, z) = b_{v_s}(x, y, z)\boldsymbol{v}(x, y, z). \tag{44}$$

The finite element formulation separately reconstructs $\boldsymbol{v}_c(x,y,z)$ and $\boldsymbol{v}_s(x,y,z)$ specified by Eqs. (43) and (44) respectively.

Now, the relationship between the LDV velocity data and the modeled velocity field must be obtained. This relationship is based upon the vector dot product between

the LDV velocity data and the modeled velocity field at each LDV scan point [23]. The vector dot product is

$$\boldsymbol{v}_L \cdot \boldsymbol{v} = v_{L_x} v_x + v_{L_y} v_y + v_{L_z} v_z , \tag{45}$$

where all terms are functions of *x*, *y*, *z* and *t* and v_L is the velocity vector in the direction of the laser beam whose magnitude, $|\boldsymbol{v}_L|$, is the velocity measured by the LDV. Equation (45) may also be written as

$$\boldsymbol{v}_L \cdot \boldsymbol{v} = |\boldsymbol{v}_L||\boldsymbol{v}| \cos \boldsymbol{\Phi} , \tag{46}$$

where $\boldsymbol{\Phi}$ is the angle between $\boldsymbol{v}_L$ and $\boldsymbol{v}$. Equating Eqs. (45) and (46) yields

$$v_{L_x} v_x + v_{L_y} v_y + v_{L_z} v_z = |\boldsymbol{v}_L||\boldsymbol{v}| \cos \boldsymbol{\Phi} . \tag{47}$$

Using a right-triangle relationship yields

$$\cos \boldsymbol{\Phi} = \frac{|\boldsymbol{v}_L|}{|\boldsymbol{v}|} . \tag{48}$$

Therefore, Eq. (47) becomes

$$v_{L_x} v_x + v_{L_y} v_y + v_{L_z} v_z = |\boldsymbol{v}_L||\boldsymbol{v}_L| . \tag{49}$$

Dividing Eq. (49) by $|\boldsymbol{v}_L|$ yields

$$\frac{v_{L_x}}{|\boldsymbol{v}_L|} v_x + \frac{v_{L_Y}}{|\boldsymbol{v}_L|} v_y + \frac{v_{L_z}}{|\boldsymbol{v}_L|} v_z = |\boldsymbol{v}_L| \tag{50}$$

or

$$\psi_{L_x} v_x + \psi_{L_y} v_y + \psi_{L_z} v_z = |\boldsymbol{v}_L| , \tag{51}$$

where ψ_{L_x}, ψ_{L_y} and ψ_{L_z} are direction cosines for $|\boldsymbol{v}_L|$ referenced to the structure coordinate system.

The direction cosines at each scan point must be determined before completing the velocity finite element formulation. Before explaining how this is accomplished, the manner in which surface geometry and velocity are modeled via the finite element method must be explained. Recall that ESDM begins with the creation of a finite element mesh which model surface geometry and velocity. Both surface geometry and velocity within each element domain are described with respect to nodal, Cartesian component values for these quantities in terms of known interpolating functions which depend on the parametric coordinates, ξ, η and ζ, that define location in an element. For a particular scan point i within a particular element, the variation of surface geometry within the element is

$$\begin{aligned} x_i &= \sum_{j=1}^{m} N_j(\xi_i,\eta_i,\zeta_i)x_j \\ y_i &= \sum_{j=1}^{m} N_j(\xi_i,\eta_i,\zeta_i)y_j \\ z_i &= \sum_{j=1}^{m} N_j(\xi_i,\eta_i,\zeta_i)z_j \end{aligned} \quad , \tag{52}$$

where the summation is over the number of element nodes m, $N_j(\xi_i,\eta_i,\zeta_i)$ is the interpolation function associated with the j node and x_i, y_i and z_i are the nodal Cartesian coordinate values. For the same scan point i, the variation of the Cartesian velocity field components within the element is

$$
\begin{aligned}
v_{x_i} &= \sum_{j=1}^{m} N_j(\xi_i,\eta_i,\zeta_i) v_{x_j} \\
v_{y_i} &= \sum_{j=1}^{m} N_j(\xi_i,\eta_i,\zeta_i) v_{y_j} \\
v_{z_i} &= \sum_{j=1}^{m} N_j(\xi_i,\eta_i,\zeta_i) v_{z_j}
\end{aligned}
\qquad (53)
$$

where the summation is again over the number of element nodes *m*, $N_j(\xi_i,\eta_i,\zeta_i)$ is again the interpolation function associated with the *j* node and v_{x_j}, v_{y_j} and v_{z_j} are velocity field components evaluated at the *j* node. As indicated by Eqs. (52) and (53), surface geometry and velocity interpolation functions are the same; hence the elements used by ESDM are isoparametric elements since both geometry and velocity are modeled by the same functions [24]. The form of the interpolating functions depends on the type of element used; Montgomery lists the element types used by ESDM and the corresponding interpolating functions associated with each node [25]. Presently, linear triangular, linear quadrilateral, quadratic quadrilateral, cubic quadrilateral and cubic B-spline elements are available.

The direction cosines are determined in the following manner. Recall that the primary purpose of LDV registration is to determine the pose of the LDV relative to the structure. Mathematically, registration involves calculating a transformation matrix, $[\boldsymbol{\Gamma}]_{L\rightarrow S}$, which permits coordinate transformations from LDV coordinates to structure coordinates. Once the LDV pose relative to the structure is defined, a vector describing the direction of the laser beam to a scan point on the structure is determined in the structure coordinate system. This vector is $\boldsymbol{v}_L$ in Eqs. (45) and (46). Its time-dependent

magnitude is directly obtained by the LDV during scanning. Direction is determined by the scan angles and the range which minimizes the transformation matrix, $[\boldsymbol{\Gamma}]_{L\to S}$. The scan angles define a vector direction in the LDV coordinate system from the LDV origin to the scan point. Range to the scan point is not required since only direction is required. The transformation matrix then transforms this vector to the structure coordinate system, thus defining $\boldsymbol{v}_L$. To determine the direction cosines, the vector dot product of $\bar{\boldsymbol{v}}_L$, where

$$\bar{\boldsymbol{v}}_L = \frac{\boldsymbol{v}_L}{|\boldsymbol{v}_L|}, \tag{54}$$

and $\bar{\boldsymbol{r}}_S$, where

$$\bar{\boldsymbol{r}}_S = \frac{\boldsymbol{r}_S}{|\boldsymbol{r}_S|}, \tag{55}$$

is evaluated. The vector $\boldsymbol{r}_S$ defines the position vector of a scan point in the structure coordinate system and is determined using the finite element surface geometry model. The structure coordinates of the surface geometry element nodes are known. Recall that surface geometry variation within each element is described by interpolating functions and these interpolating functions depend on parametric coordinates which define the scan point location in each element. The form of these interpolating functions is known; however, the actual parametric coordinate values that define the scan point location are not known. These values must be determined before a scan point position vector can be defined. From Eq. (52), the location of a scan point within an element is

$$x_i = \sum_{j=1}^{m} N_j(\xi_i, \eta_i, \zeta_i) x_j$$
$$y_i = \sum_{j=1}^{m} N_j(\xi_i, \eta_i, \zeta_i) y_j \,. \tag{56}$$
$$z_i = \sum_{j=1}^{m} N_j(\xi_i, \eta_i, \zeta_i) z_j$$

The only unknown values in this equation are the parametric coordinate values ξ_i, η_i and ζ_i. The scan point coordinate values x_i, y_i and z_i, the nodal coordinate values x_j, y_j and z_j and the form of the interpolation functions $N_j(\xi_i,\eta_i,\zeta_i)$, are all known. Therefore, the parametric coordinate values ξ_i, η_i and ζ_i of each scan point may be determined after proper rearrangement of the equations represented by Eq. (56) [26]. Once this is accomplished, scan point position vectors referenced to the structure coordinate system are obtained. Then, the direction cosines, ψ_{L_x}, ψ_{L_y} and ψ_{L_z}, are determined by evaluating the dot product between $\bar{\boldsymbol{v}}_L$ and $\bar{\boldsymbol{r}}_S$.

As mentioned before, the velocity finite element formulation used by ESDM depends on a weighted, least-squares approach; this approach entails minimization of the squared error between LDV velocity data and the modeled velocity field at each LDV scan point, all weighted by the residual error variance obtained from the velocity response time-domain regressions. With the aid of Eqs. (21) and (51), the error between LDV velocity data and the modeled velocity field at each scan point is

$$e_i = \psi_{L_{x_i}} v_{x_i} + \psi_{L_{y_i}} v_{y_i} + \psi_{L_{z_i}} v_{z_i} - \left|\boldsymbol{v}_L\right|. \tag{57}$$

Therefore, the squared error is

$$e_i^2 = \left(\psi_{L_{x_i}} v_{x_i} + \psi_{L_{y_i}} v_{y_i} + \psi_{L_{z_i}} v_{z_i} - \left|\mathbf{v}_L\right|\right)^2, \tag{58}$$

and the squared error at each scan point weighted by the corresponding residual error variance is

$$\frac{e_i^2}{\sigma_i^2} = \frac{\left(\psi_{L_{x_i}} v_{x_i} + \psi_{L_{y_i}} v_{y_i} + \psi_{L_{z_i}} v_{z_i} - \left|\mathbf{v}_L\right|\right)^2}{\sigma_i^2}. \tag{59}$$

Summing the weighted, squared errors over all scan points in a single element yields

$$\Pi = \sum_{i=1}^{n} \frac{e_i^2}{\sigma_i^2} \tag{60}$$

or

$$\boldsymbol{\Pi} = \sum_{i=1}^{n} \frac{\left(\psi_{L_{x_i}} v_{x_i} + \psi_{L_{y_i}} v_{y_i} + \psi_{L_{z_i}} v_{z_i} - \left|\mathbf{v}_L\right|\right)^2}{\sigma_i^2}. \tag{61}$$

This equation provides the basis for the following finite element formulation [27].

The finite element formulation involves minimization of Eq. (61) with respect to each of the unknown nodal velocity field components [28]. Via Eq. (53), Eq. (61) is written in terms of nodal velocity field components as

$$\boldsymbol{\Pi} = \sum_{i=1}^{n} \frac{\left(\psi_{L_{x_i}} \sum_{j=1}^{m} N_{ji} v_{x_j} + \psi_{L_{y_i}} \sum_{j=1}^{m} N_{ji} v_{y_j} + \psi_{L_{z_i}} \sum_{j=1}^{m} N_{ji} v_{z_j} - \left|\mathbf{v}_{L_i}\right|\right)^2}{\sigma_i^2}, \tag{62}$$

where

$$N_{ji} = N_j\left(\xi_i, \eta_i, \zeta_i\right). \tag{63}$$

To simplify upcoming mathematical operations, Eq. (62) is written as

$$\Pi = \sum_{i=1}^{n} \frac{\left[e_i\left(v_{x_j}, v_{y_j}, v_{z_j}\right)\right]^2}{\sigma_i^2}, \tag{64}$$

where

$$e_i\left(v_{x_j}, v_{y_j}, v_{z_j}\right) = \psi_{L_{x_i}} \sum_{j=1}^{m} N_{ji} v_{x_j} + \psi_{L_{y_i}} \sum_{j=1}^{m} N_{ji} v_{y_j} + \psi_{L_{z_i}} \sum_{j=1}^{m} N_{ji} v_{z_j} - \left|\boldsymbol{v}_{L_i}\right|. \tag{65}$$

Minimization implies evaluating the partial derivative of Eq. (64) with respect to each of the nodal velocity field components and setting the result equal to zero. This operation yields

$$\begin{aligned}
\frac{\partial \Pi}{\partial v_{x_j}} &= 2\sum_{i=1}^{n} \frac{e_i\left(v_{x_j}, v_{y_j}, v_{z_j}\right)}{\sigma_i^2} \frac{\partial}{\partial v_{x_j}} \left[e_i\left(v_{x_j}, v_{y_j}, v_{z_j}\right)\right] \\
\frac{\partial \Pi}{\partial v_{y_j}} &= 2\sum_{i=1}^{n} \frac{e_i\left(v_{x_j}, v_{y_j}, v_{z_j}\right)}{\sigma_i^2} \frac{\partial}{\partial v_{y_j}} \left[e_i\left(v_{x_j}, v_{y_j}, v_{z_j}\right)\right] \\
\frac{\partial \Pi}{\partial v_{z_j}} &= 2\sum_{i=1}^{n} \frac{e_i\left(v_{x_j}, v_{y_j}, v_{z_j}\right)}{\sigma_i^2} \frac{\partial}{\partial v_{z_j}} \left[e_i\left(v_{x_j}, v_{y_j}, v_{z_j}\right)\right]
\end{aligned} \tag{66}$$

or

$$\begin{aligned}
\frac{\partial \Pi}{\partial v_{x_j}} &= \sum_{i=1}^{n} \frac{\sum_{j=1}^{m} N_{ji} \psi_{L_{x_i}} \left[N_{ji}\left(\psi_{L_{x_i}} v_{x_j} + \psi_{L_{y_i}} v_{y_j} + \psi_{L_{z_i}} v_{z_j}\right) - \left|\boldsymbol{v}_L\right|\right]^2}{\sigma_i^2} \\
\frac{\partial \Pi}{\partial v_{y_j}} &= \sum_{i=1}^{n} \frac{\sum_{j=1}^{m} N_{ji} \psi_{L_{y_i}} \left[N_{ji}\left(\psi_{L_{x_i}} v_{x_j} + \psi_{L_{y_i}} v_{y_j} + \psi_{L_{z_i}} v_{z_j}\right) - \left|\boldsymbol{v}_L\right|\right]^2}{\sigma_i^2} \\
\frac{\partial \Pi}{\partial v_{z_j}} &= \sum_{i=1}^{n} \frac{\sum_{j=1}^{m} N_{ji} \psi_{L_{z_i}} \left[N_{ji}\left(\psi_{L_{x_i}} v_{x_j} + \psi_{L_{y_i}} v_{y_j} + \psi_{L_{z_i}} v_{z_j}\right) - \left|\boldsymbol{v}_L\right|\right]^2}{\sigma_i^2}
\end{aligned}. \tag{67}$$

In matrix form for element *k*, Eq. (67) yields

$$[\boldsymbol{K}]_k \boldsymbol{v}_k = \boldsymbol{f}_k, \tag{68}$$

where

$$[\mathbf{K}]_k = \sum_{i=1}^{n} \begin{bmatrix} N_{1i}^2\psi_{L_{x_i}}^2 & N_{1i}^2\psi_{L_{x_i}}\psi_{L_{y_i}} & N_{1i}^2\psi_{L_{x_i}}\psi_{L_{y_i}} & \cdots & N_{1i}N_{mi}\psi_{L_{x_i}}\psi_{L_{z_i}} \\ & N_{1i}^2\psi_{y_i}^2 & N_{1i}^2\psi_{L_{y_i}}\psi_{L_{z_i}} & \cdots & N_{1i}N_{mi}\psi_{L_{y_i}}\psi_{L_{z_i}} \\ & & N_{1i}^2\psi_{L_{z_i}}^2 & \cdots & N_{1i}N_{mi}\psi_{L_{z_i}}^2 \\ & \text{symmetric} & & & \vdots \\ & & & & N_{mi}^2\psi_{L_{z_i}}^2 \end{bmatrix}_k, \tag{69}$$

$$\boldsymbol{v}_k = \begin{Bmatrix} v_{x_1} \\ v_{y_1} \\ v_{z_1} \\ \vdots \\ v_{z_m} \end{Bmatrix}_k \tag{70}$$

and

$$\boldsymbol{f}_k = \sum_{i=1}^{n} \begin{Bmatrix} N_{1i}\psi_{L_{x_i}} \left|\boldsymbol{v}_{L_i}\right| \\ N_{1i}\psi_{L_{y_i}} \left|\boldsymbol{v}_{L_i}\right| \\ N_{1i}\psi_{L_{z_i}} \left|\boldsymbol{v}_{L_i}\right| \\ \vdots \\ N_{1m}\psi_{L_{z_m}} \left|\boldsymbol{v}_{L_i}\right| \end{Bmatrix}_k . \tag{71}$$

$[\boldsymbol{K}]_k$ is a known symmetric matrix termed the *element effective dynamic stiffness matrix*, $\boldsymbol{v}_k$ is an unknown vector of nodal velocity field components and $\boldsymbol{f}_k$ is a known vector termed the *effective nodal force vector* [29]. Compared with traditional static and dynamic structural finite element formulations, $[\boldsymbol{K}]_k$ is analogous to the element stiffness matrix, $\boldsymbol{v}_k$ is analogous to the unknown nodal displacement vector and $\boldsymbol{f}_k$ is analogous to the known nodal force vector.

Equation (68) is the ESDM finite element formulation for a single element containing n scan points. Next, the formulations for all l elements are assembled to create the velocity field finite element model. The assembled finite element model is

$$[\boldsymbol{K}]\boldsymbol{v} = \boldsymbol{f}\ , \tag{72}$$

where $[\boldsymbol{K}]$ is the assembled effective dynamic stiffness matrix composed of l individual matrices $[\boldsymbol{K}]_k$, $\boldsymbol{v}$ is the assembled nodal velocity field component vector composed of l individual vectors $\boldsymbol{v}_k$ and $\boldsymbol{f}$ is the assembled effective nodal force vector composed of l individual $\boldsymbol{f}_k$. As with traditional assembled, or global, stiffness matrices, the effective dynamic stiffness matrix, $[\boldsymbol{K}]$, is positive definite, symmetric and banded with a majority of its elements near the main diagonal [30]. Since $[\boldsymbol{K}]$ is positive definite and symmetric, its inverse exists [31]. Therefore, solving for the nodal velocity field component vector containing the unknown velocity field components at the element nodes yields

$$\boldsymbol{v} = [\boldsymbol{K}]^{-1}\boldsymbol{f}\ . \tag{73}$$

Once the nodal velocity field components are obtained, the element interpolating functions can be used to determine the continuous, three-dimensional velocity field.

Recall that the modeled velocity field may be separated into real cosine and sine components as indicated by Eq. (42). Therefore, as Montgomery demonstrates [32], Eq. (51) is separated into independent cosine and sine components as

$$\psi_{L_x} v_{x_c} + \psi_{L_y} v_{y_c} + \psi_{L_z} v_{z_c} = \left|\boldsymbol{v}_{L_c}\right| \tag{74}$$

and

$$\psi_{L_x} v_{x_s} + \psi_{L_y} v_{y_s} + \psi_{L_z} v_{z_s} = \left|\boldsymbol{v}_{L_s}\right|, \tag{75}$$

where

$$\left|\boldsymbol{v}_{L_c}\right| = b_{v_c} \tag{76}$$

and

$$\left|\boldsymbol{v}_{L_s}\right| = b_{v_s} . \tag{77}$$

Consequently, the cosine and sine components are solved independently by a separate, yet identical, ESDM finite element formulation for each cosine and sine component. This yields solutions for $\boldsymbol{v}_c(x,y,z)$ and $\boldsymbol{v}_s(x,y,z)$ via Eq. (73). These separate solutions are combined to yield the continuous, three-dimensional velocity field given by

$$\boldsymbol{v}(x,y,z,t) = \boldsymbol{v}_c(x,y,z)\cos(\omega t) + \boldsymbol{v}_s(x,y,z)\sin(\omega t). \tag{78}$$

As a result, the overall velocity field solution, consisting of the cosine and sine components, retain continuous, three-dimensional phase information referenced to the excitation. Of course, continuous continuous, three-dimensional magnitude information is also retained.

Velocity Field Solution Processing

Once the velocity field solution is obtained, the residual error between the LDV velocity data and the velocity field solution is obtained; the ratio between velocity magnitude and residual error at each scan point is also calculated [33].

The velocity field obtained using the ESDM finite element formulation via Eq. (73) is a translational field. An angular velocity field also exists which may be obtained by evaluating the vector curl of the translational velocity field solution and dividing by two [34].

The velocity field solution is

$$\boldsymbol{v}(x,y,z,t) = \boldsymbol{v}_c(x,y,z)\cos(\omega t) + \boldsymbol{v}_s(x,y,z)\sin(\omega t) \tag{79}$$

or

$$\boldsymbol{v}(x,y,z,t) = \boldsymbol{v}(x,y,z)\cos(\omega t - \phi_r), \tag{80}$$

where now

$$\boldsymbol{v}(x,y,z) = \sqrt{\boldsymbol{v}_c(x,y,z)^2 + \boldsymbol{v}_s(x,y,z)^2} \tag{81}$$

and

$$\phi_r = \tan^{-1}\left[\frac{\boldsymbol{v}_s(x,y,z)}{\boldsymbol{v}_c(x,y,z)}\right]. \tag{82}$$

Therefore, using Eq. (80), the translational displacement field is

$$\boldsymbol{d}(x,y,z,t) = \int \boldsymbol{v}(x,y,z,t)dt = \int \boldsymbol{v}(x,y,z)v(t)dt = \boldsymbol{v}(x,y,z)\int v(t)dt \tag{83}$$

or

$$\boldsymbol{d}(x,y,z,t) = \boldsymbol{v}(x,y,z)\int \cos[\omega t - \phi_r(x,y,z)]\,dt = \frac{\boldsymbol{v}(x,y,z)}{\omega}\sin[\omega t - \phi_r(x,y,z)]. \tag{84}$$

Equation (84) is exact. No functions or constants of integration need be evaluated if Eq. (84) is evaluated over a complete period since the response is steady-state and harmonic. Similarly, the angular diplacement field may be determined by integrating the angular velocity field. The translational acceleration field is

$$\boldsymbol{a}(x,y,z,t) = \frac{\partial \boldsymbol{v}(x,y,z,t)}{\partial t} = \frac{\partial[\boldsymbol{v}(x,y,z)v(t)]}{\partial t} = \boldsymbol{v}(x,y,z)\frac{d[v(t)]}{dt} \tag{85}$$

or

$$\boldsymbol{a}(x,y,z,t) = \boldsymbol{v}(x,y,z)\frac{d[\cos(\omega t - \phi)]}{dt} = \omega \boldsymbol{v}(x,y,z)\cos(\omega t - \phi_r). \tag{86}$$

Likewise, differentiating the angular velocity field with respect to time yields the angular acceleration field. Also, as discussed by Montgomery [35], the strain field may be obtained.

ESDM Software

Several computer programs are included with the ESDM software suite. These programs contain algorithms which compute the LDV transformation matrix $[\boldsymbol{\Gamma}]_{L\rightarrow S}$, direct the LDV laser beam, collect velocity data at each scan point, perform the time-signal regression, reconstruct the translational velocity field, compute other related fields and display all results.

ESDM employs powerful display software which allows color visualization of velocity and related fields. Magnitude, phase and direction information associated with these fields may be displayed and animated from various structure viewpoints. In addition, statistical information regarding the velocity field solution may be displayed.